ISSN: 2414-1895 DOI: 10.6919/ICJE.202504_11(4).0025

Coupling of Fabry–Pérot Cavity and Metallic Nanograting Array for High-Quality-Factor Plasmonic Modes

Yufan Ye

Guangdong University of Technology, Guangzhou, 510006, China

Abstract

The quality (Q) factors of surface plasmons (SPs) is crucial for enhancing optical field localization and optimizing the performance of optical devices, offering broad potential applications in nanolasers, photonic sensing, and nonlinear optics. To further improve the Q factors of SP modes and achieve efficient modal control, this study proposes a composite structure that integrates a Fabry–Pérot (FP) cavity with a metallic nanograting array. By leveraging the strong coupling between the resonant modes of the FP cavity and the plasmonic resonances of the grating array, the structure induces Fano resonance, thereby realizing plasmonic modes with narrow linewidths and high Q factors. The results demonstrate that this composite system can achieve a Q factor as high as 182.5 when the FP cavity thickness is 700 nm and maintains a stable high Q factors within the cavity thickness range of 670-750 nm. Moreover, the introduction of the FP cavity not only optimizes the radiation loss of the plasmonic modes but also provides a flexible means of spectral tuning. By adjusting the geometric parameters of the FP cavity, the resonance behavior of the plasmon-cavity modes can be effectively controlled, offering a novel strategy for designing high-performance nanophotonic devices. This high-Q plasmonic platform holds significant application value in nanophotonics, on-chip photonics, and high-sensitivity sensing.

Keywords

Surface Plasmons; Fabry-Pérot Cavity; Quality Factor.

1. Introduction

Surface plasmons (SPs) are a crucial research subject in the field of micro-nano optics, embodying the key physical mechanisms of light-metal interactions. At the micro-nano scale, the coupling between SPs and light exhibits rich electromagnetic properties, enabling highly controllable optical field modulation [1,2]. This characteristic not only surpasses the diffraction limit to achieve nanoscale optical field localization but also endows SPs with broad application prospects in surface plasmon nanolasers [3,4], subwavelength imaging [5], high-sensitivity sensing [6], nonlinear optics [7], quantum information processing [8] and biosensing [9,10].

The inherent Ohmic loss and high far-field radiation of metallic materials severely constrain the Q factors of surface plasmons, thereby limiting their practical applications in high-precision optical devices. Studies have shown that by rationally designing periodic metallic nanoparticle arrays, radiation losses can be effectively reduced, leading to an enhancement in the Q factors of SPs. However, most existing studies remain constrained by relatively low Q factors, or their structural designs lack flexibility, making it challenging to maintain a stable high Q factors over a broad spectral range. To address this issue, this study proposes the integration of an optical nanocavity structure, where optimizing cavity design further enhances the performance of SPs. Therefore, the rational design of optical nanocavities and the realization of high-Q plasmonic mode coupling remain crucial research topics.

ISSN: 2414-1895 DOI: 10.6919/ICJE.202504_11(4).0025

In this study, we introduce a Fabry-Pérot (FP) cavity into a metallic nanograting array and propose a high-Q factor optical nanocavity physical model based on the coupling between SPs and the FP cavity. By tuning the cavity length of the FP cavity, strong coupling between SPs and FP cavity modes is achieved, effectively suppressing radiation loss and narrowing the resonance linewidth, thereby significantly enhancing the Q factors. Further analysis demonstrates that this coupling mechanism enables the realization of a surface plasmon nanocavity with a Q factor as high as 182.5, while maintaining a Q factor above 100 within a cavity thickness range of 670-750 nm, showcasing excellent structural stability and application potential. This design effectively reduces radiation loss and enhances the Q factors of SPs, providing new insights for the development of high-performance nanophotonic devices. It holds significant application value in optoelectronics [11], nanolasers, and on-chip integrated photonics [12,13].

2. Results and Discussion

This study proposes a structure that combines an FP cavity with a metallic nanograting array, achieving a high Q factors through the coupling between plasmons and FP cavity modes. The FP cavity consists of two metallic reflectors, with a dielectric layer of refractive index $n = 1.46$ in between. Figure 1(a) presents the reflection spectra of the FP cavity under normal incidence for different cavity lengths T. The results indicate that as T increases, the resonance wavelength of the FP cavity monotonically shifts to longer wavelengths. A two-dimensional grating array with a honeycomb-like topological structure is constructed by periodically arranging triangular metallic nanoparticles with a side length of approximately 279 nm on the dielectric layer (Figure 1(b)). The reflection spectrum of this structure reveals that a localized surface plasmon resonance (LSPR) occurs at 1116 nm, with a full-width at half-maximum (FWHM) of 108.25 nm, indicating that the system still exhibits relatively high radiation losses.

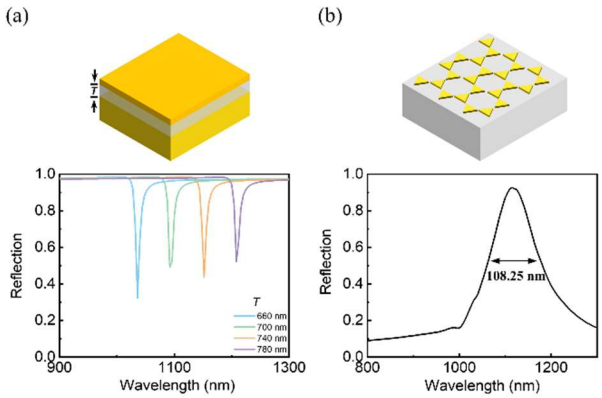

Figure 1. Schematic diagram of the structure and spectral characteristics under normal incidence. (a) FP cavity. (b) Periodic triangular nanoparticle array arranged on a dielectric layer. The upper layer of the FP cavity is silver, the lower layer is gold, and the nanoparticle array is composed of silver.

Introducing an optical nanocavity into a periodic nanograting array structure can significantly alter its optical response characteristics. Figure 2(a) schematically illustrates the basic geometric configuration of this composite structure, where a metallic substrate is added beneath the nanograting array shown in Figure 1(b). The incident light is normally incident along the $-z$ direction and polarized along the x direction. Figure 2(b) presents the reflection spectrum of this structure, where the orange curve represents the interaction between surface plasmons and the optical nanocavity when the cavity thickness T is 700 nm. It can be observed that the optical cavity induces significant modifications, particularly in the spectral response, resulting in a narrow linewidth of 6.02 nm. Near the reflection dip at a wavelength of 1104 nm, the high-radiation-loss surface plasmon mode appears as a

ISSN: 2414-1895 DOI: 10.6919/ICJE.202504_11(4).0025

Lorentzian-shaped resonance (black curve), which couples with the narrow resonance of the FP cavity (green curve) to form a characteristic Fano resonance profile. Furthermore, at this point, the surface plasmon resonance peak is located at 1116 nm (on the red side of the Fano resonance), while the narrow FP cavity resonance peak appears at 1093 nm (on the blue side of the Fano resonance). The asymmetric coupling between these two electromagnetic resonances of different strengths gives rise to the Fano resonance peak. By carefully designing and tailoring the lineshape and relative position of these resonance peaks, efficient modal coupling can be achieved, leading to an even narrower resonance linewidth and a further enhanced Q factors. Ultimately, a high Q factor of approximately 182.5 is realized.

Figure 2 illustrates the interaction between localized surface plasmons (LSPs) and the FP cavity, along with its tuning mechanism. As shown in Figure 2(c), different cavity thicknesses correspond to distinct spectral responses. With increasing T, the Fano resonance peak undergoes a redshift, accompanied by a series of lineshape variations. When T = 660 nm and T = 700 nm, the resonance profile remains asymmetric: the blue-side peak exhibits strong attenuation, while the red-side attenuation is more gradual. This corresponds to the locations of the FP cavity and plasmonic resonance modes, with the former on the blue side and the latter on the red side. At T = 660 nm, the reflection dip falls below 20%, whereas at T = 700 nm, it rises to approximately 40%, indicating a decrease in modulation depth during this transition. As the cavity thickness further increases to T = 740 nm and T = 780 nm, the asymmetric Fano resonance lineshape reappears. However, at this stage, the blue-side peak variation becomes more gradual, while the red-side variation becomes more pronounced, in contrast to the profiles observed at T = 660 nm and T = 700 nm. Meanwhile, the surface plasmon resonance shifts to the blue side, whereas the FP cavity resonance shifts to the red side. This results in a symmetric relationship between T = 700 nm and T = 740 nm, as well as between T = 660 nm and T = 780 nm. Given that the surface plasmon resonance is located at a wavelength of 1116 nm, it is evident that the interaction between SPs and FP cavity resonance is not a simple superposition but rather a complex and unpredictable hybridization effect, arising from phase-induced coherence. In other words, the relative spectral position of the FP cavity resonance and the plasmonic resonance can lead to either constructive or destructive interference, manifesting as Fano resonance lineshapes. When constructive interference is maximized, the hybridized mode disappears, leaving only the FP cavity characteristics. As shown in Figure 2(b), the spectrum for T = 700 nm is represented by the orange solid line, which can be decomposed into the cavity mode and the plasmonic mode, represented by the green and black solid lines, respectively.

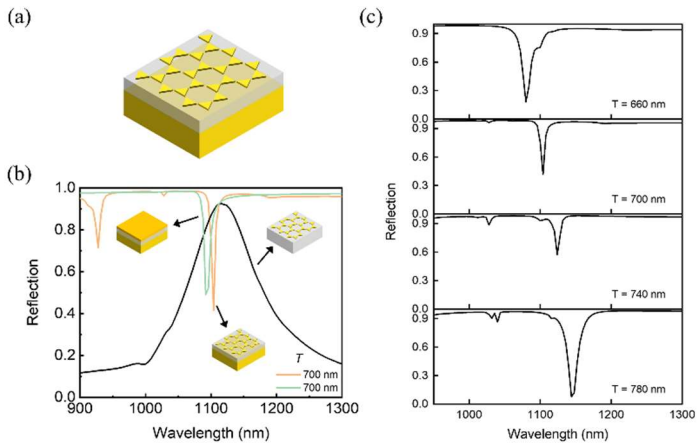

Figure 2. (a) Schematic diagram of the structure. (b) Spectral characteristics of the structure at a cavity thickness T = 700 nm under normal incidence. (c) Spectral characteristics of the hybrid structure at different cavity thicknesses.

ISSN: 2414-1895 DOI: 10.6919/ICJE.202504_11(4).0025

Figure 3 illustrates the relationship between the optical nanocavity thickness, Q factor, and resonance wavelength. The blue curve indicates a proportional relationship between cavity thickness and resonance wavelength. As T increases from 630 nm, the resonance wavelength undergoes a redshift, consistent with the FP cavity mode behavior. When the cavity thickness reaches 720 nm, the coupling between the LSP mode of the array and the FP cavity mode vanishes. At this point, the plasmonic effect is at its weakest, and only the resonance response of the FP cavity remains. The Q factor is closely related to the surface plasmon resonance wavelength. As shown in Figure 3, within the cavity thickness range of $T < 720$ nm, the Q factor increases as T increases and the Fano resonance undergoes a redshift. The maximum Q factor of 182.5 is achieved at $T = 700$ nm. In correspondence with the discussion in Figure 2, throughout this process, the surface plasmon resonance remains fixed at 1116 nm, whereas the FP cavity resonance continuously redshifts with increasing T, leading to a shift in the Fano mode. As the FP cavity mode gradually approaches the surface plasmon mode, the coupling strength rapidly increases, resulting in an enhanced Q factor. However, for $T > 720$ nm, further increasing T causes the optical cavity mode to shift further toward longer wavelengths, resulting in a continued redshift of the Fano mode. As the optical cavity mode moves away from the surface plasmon resonance, the coupling gradually weakens, leading to a progressive decline in the Q factor. At $T = 720$ nm, the coupling between the surface plasmon mode and the optical cavity mode disappears, and the reflection behavior of the triangular gold nanoparticle array becomes identical to that of the metal film, indicating that the coherent enhancement of the FP cavity mode reaches its maximum.

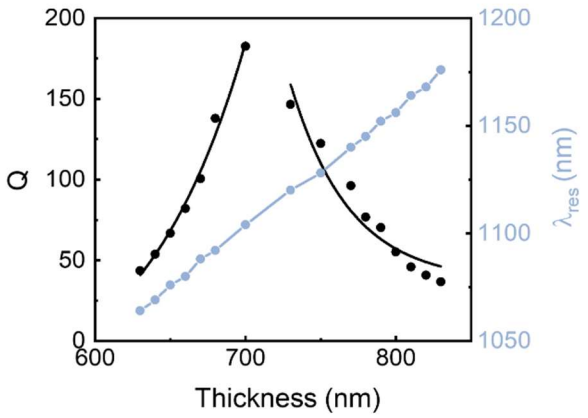

Figure 3. The relationship between the optical nanocavity thickness, Q factor, and resonance wavelength in the hybrid structure.

3. Summary

In summary, this study proposes a hybrid structure that combines a FP cavity with a metallic nanograting array and systematically investigates the strong coupling effect between plasmonic modes and optical nanocavities. By introducing an optical nanocavity into a conventional periodic nanograting array, the Q factor of SPs is significantly enhanced, enabling highly efficient optical field modulation. The results demonstrate that this structure maintains a high and stable Q factor over a broad spectral range while exhibiting excellent spectral tuning capabilities. Future research can further explore the tunability of this structure over a wider spectral range, as well as the influence of different metallic materials, nanoparticle geometries, and dielectric layer parameters on the Q factor. Additionally, integrating nonlinear optical effects or quantum optical mechanisms may further optimize optical field control, offering new strategies for the development of high-performance plasmonic optical devices. This study not only advances the functionalization and application of plasmonic nanostructures in optoelectronics and sensing but also provides new insights into the design of high-Q factor functional nanostructures.

ISSN: 2414-1895 DOI: 10.6919/ICJE.202504_11(4).0025

References

[1] WANG P, KRASAVIN A V, LIU L, et al. Molecular plasmonics with metamaterials. Chemical Reviews, 2022, 122(19): 15031-15081.

[2] WINKLER J M, RUCKRIEGEL M J, ROJO H, et al. Dual-wavelength lasing in quantum-dot plasmonic lattice lasers. ACS Nano, 2020, 14(5): 5223-5232.

[3] JUN L, ZHEN H, CHIA WU, et al. Highly Localized Surface Plasmon Nanolasers via Strong Coupling. Nano Lett., 2023, 23(10): 1530-6984.

[4] LIANG Y, LI C, HUANG Y-Z, et al. Plasmonic nanolasers in on-chip light sources: Prospects and challenges. ACS Nano, 2020, 14(11): 14375-14390.

[5] HU J, WANG D, BHOWMIK D, et al. Lattice-resonance metalenses for fully reconfigurable imaging. ACS Nano, 2019, 13(4): 4613-4620.

[6] KARAWDENIYA B I, DAMRY A M, MURUGAPPAN K, et al. Surface functionalization and texturing of optical metasurfaces for sensing applications. Chemical Reviews, 2022, 122(19): 14990-15030.

[7] ZHI C, MERCEDEH K, GUO C, et al. Nonlinear Optics: feature issue introduction. Opt. Express, 2024, 32, 20862-20865.

[8] XU D, XIONG X, WU L, et al. Quantum plasmonics: New opportunity in fundamental and applied photonics. Advances in Optics and Photonics, 2018, 10(4): 703-756.

[9] MOGERA U, GUO H, NAMKOONG M, et al. Wearable plasmonic paper-based microfluidics for continuous sweat analysis. Science Advances, 2022, 8(12): 1736.

[10] [CHEN G, XIAO X, ZHAO X, et al. Electronic textiles for wearable point-of-care systems. Chemical Reviews, 2022, 122(3): 3259-3291.

[11] ELBANNA A, JIANG H, FU Q, et al. 2D material infrared photonics and plasmonics. ACS Nano, 2023, 17(5): 4134-4179.

[12] ASHTIANI F, GEERS A J, AFLATOUNI F. An on-chip photonic deep neural network for image classification. Nature, 2022, 606(7914): 501-506.

[13] YAN T, YANG R, ZHENG Z, et al. All-optical graph representation learning using integrated diffractive photonic computing units. Science Advances, 2022, 8(24): 7630.